The AAPS Journal (2019) 21: 12
DOI: 10.1208/s12248-018-0285-7

Research Article

Evaluation of a Particulate Breast Cancer Vaccine Delivered *via* Skin

Lipika Chablani,[1,5] Suprita A. Tawde,[2] Archana Akalkotkar,[3] and Martin J. D'Souza[4]

Received 30 August 2018; accepted 11 December 2018; published online 2 January 2019

Abstract. Breast cancer impacts female population globally and is the second most common cancer for females. With various limitations and adverse effects of current therapies, several immunotherapies are being explored. Development of an effective breast cancer vaccine can be a groundbreaking immunotherapeutic approach. Such approaches are being evaluated by several clinical trials currently. On similar lines, our research study aims to evaluate a particulate breast cancer vaccine delivered *via* skin. This particulate breast cancer vaccine was prepared by spray drying technique and utilized murine breast cancer whole cell lysate as a source of tumor-associated antigens. The average size of the particulate vaccine was 1.5 μm, which resembled the pathogenic species, thereby assisting in phagocytosis and antigen presentation leading to further activation of the immune response. The particulate vaccine was delivered *via* skin using commercially available metal microneedles. Methylene blue staining and confocal microscopy were used to visualize the microchannels. The results showed that microneedles created aqueous conduits of 50 ± 10 μm to deliver the microparticulate vaccine to the skin layers. Further, an *in vivo* comparison of immune response depicted significantly higher concentration of serum IgG, IgG2a, and B and T cell (CD4+ and CD8+) populations in the vaccinated animals than the control animals ($p < 0.001$). Upon challenge with live murine breast cancer cells, the vaccinated animals showed five times more tumor suppression than the control animals confirming the immune response activation and protection ($p < 0.001$). This research paves a way for individualized immunotherapy following surgical tumor removal to prolong relapse episodes.

KEY WORDS: microparticle; spray drying; whole cell lysate; microneedle; immunotherapy.

INTRODUCTION

Breast cancer impacts female population globally and is a major cause of mortality. It is the second most common cancer in women after skin cancer. National Cancer Institute (NCI) estimates 266,120 new cases of breast cancer in 2018 and an estimated death count of over 40,000 patients due to breast cancer. Several therapies are available for breast cancer patients including surgery, chemotherapy, and radiation. However, most of these conventional therapies pose various limitations and lead to significant adverse effects. To address these challenges, alternate therapies are being explored.

Lately, the focus of oncology researchers has shifted towards immunotherapy in an attempt to find a better line of treatment, which can be well tolerated by cancer patients (1,2). These immunotherapies include the use of targeted antibodies such as trastuzumab and pertuzumab. Both the antibodies are capable of targeting the overly expressed human epidermal growth factor receptor 2 (HER2) on breast cancer cells leading to an immune response against the tumor. These antibodies are good therapeutic approaches for patients whose tumors overexpress the HER2 antigen. However, if the patient's tumor does not express the HER2 antigen, not many immunotherapeutic options are available for them. As an alternative, various researchers are evaluating the use of cancer vaccines to support the unmet needs of such patients. Currently, there are over 100 clinical trials in active/recruiting/completion phases aiming to develop and clinically evaluate a breast cancer vaccine. Several delivery systems and routes of administrations are being explored for such vaccines (3–5). On similar lines, this study aims to evaluate a particulate breast cancer vaccine delivered *via* the skin in a pre-clinical murine model.

[1] Department of Pharmaceutical Science, Wegmans School of Pharmacy, St. John Fisher College, 3690 East Ave., Rochester, New York 14618, USA.
[2] Research and Development, Nexus Pharmaceuticals, Vernon Hills, Illinois 60061, USA.
[3] Charles River Laboratories, 1407 George Rd., Ashland, Ohio 44805, USA.
[4] Vaccine Nanotechnology Laboratory, Department of Pharmaceutical Sciences, College of Pharmacy and Health Sciences, Mercer University, Atlanta, Georgia 30341, USA.
[5] To whom correspondence should be addressed. (e–mail: lchablani@sjfc.edu)

The skin provides a unique site for vaccination purpose as it is easily accessible and houses various immune cells for an efficient immune response against a range of antigens. Skin serves as a barrier against multiple pathogens and is equipped with the skin-associated lymphoid tissues (SALT) to combat any insult from invading pathogens (6). Different skin cells assist in the generation of an effective immune response. Keratinocytes are the most pre-dominant (95%) epidermal cells in the skin. They can be activated by pathogens and result in the production of cytokines, which in turn recruits dendritic cells/antigen-presenting cells to the site of action leading to initiation of the immune response. Langerhans cells are a special kind of dendritic cells found in the epidermal skin layer, which are capable of immune cell activation. Langerhans cells comprise of only 2% of the total cell population in the epidermis; however, due to their extended dendrites, they spread in the epidermal layer and cover over 25% of the skin surface (7). These professional phagocytic cells provide efficient immune surveillance and further signaling to the immune cells present in their vicinity. Naturally activated dendritic/Langerhans cells mature and migrate to the draining lymph nodes. Antigens are presented at these lymph nodes *via* the major histocompatibility complexes (MHC I/II) to stimulate both T-helper (CD4+) and T-cytotoxic (CD8+) cells. Thus, Langerhans cells are responsible for activation of adaptive immune responses and can potentially generate memory response for the cancer antigens for future encounters, avoiding a chance of relapse.

Here, in this study, we explore the potential of generating a protective immune response by delivering the breast cancer antigens to the skin layers using the microneedle technology (8,9). Microneedles, as the name indicates, are micron-sized needles, which upon insertion into the skin result in the formation of aqueous conduits forming a passage for the vaccine antigens towards the immune-competent skin layers (10–12). Unlike the hypodermic needles, the microneedles are a smaller and are minimally invasive; thus, they cause limited local injection site myalgia (13). There are several types of microneedles reported in the literature, including solid, coated, hollow, and dissolving microneedles. Further, the fabrication of these microneedles can be done using various materials such as metal, silicone, glass, and maltose. Application of microneedles ranges from delivery of low molecular weight drug molecules such as lidocaine and naltrexone to delivery of biotherapeutics such as insulin and human growth hormone (14). In 2014, FDA approved Fluzone® (by Sanofi Pasteur), an intradermal influenza vaccine that incorporates a 1.5-mm needle attached to a pre-filled syringe loaded with influenza antigens. It has been shown to be efficacious when compared with an intramuscular flu vaccine, thus bringing a switch from hypodermic needles to "micro"needles for immunizations (15). Fluzone® like Sanofi's other two intradermal vaccines (IDFlu® and Intanza®) utilizes Becton and Dickinsons' Soluvia® microneedle. Soluvia® is a single 1.5-mm hollow microneedle that is attached to a syringe to deliver influenza vaccine *via* the intradermal route. This opens a new avenue of vaccine delivery through an effective, minimally invasive, and patient-friendly route of administration.

The success of immunization *via* skin using microneedles propelled us to analyze the potential of delivering a breast cancer vaccine through this route. In this study, we examine the immune response generated to a particulate breast cancer vaccine administered with the aid of microneedles in a murine model. A commercially available microneedle patch, AdminPatch® 1200, was used to deliver the particulate vaccine. AdminPatch® microneedle patches have been successfully evaluated by others as well for drug delivery applications *via* skin (16–18). Murine breast cancer 4T07 cell line was chosen as a model due to its intermediate metastatic properties compared to 67NR and 4T1 murine cell lines. Widely studied 4T07 cell line is a highly tumorigenic cell line and is capable of forming primary solid tumors at the site of injection without causing visible metastasis (19). The current study modestly aims to evaluate the role of a whole cell lysate vaccine for such a model. The 4T07 cell line was used to prepare a whole cell lysate to formulate a particulate vaccine by the spray drying technique (19–21). The whole cell lysate provides a mixture of tumor-associated antigens (TAAs) as a source for the vaccine, and this approach has been established for vaccine preparation by several others (22–24). Also, the use of spray drying technique is well known for the formulation of particulate drug delivery systems, providing a reproducible and scalable technique to the formulators (25). Hence, the study formulates the spray-dried 4T07 vaccine particles, characterizes, and evaluates the *in vitro* and *in vivo* efficacy. Further, we also describe the impact of the route of administration on immune activation with respect to our previously published work where we have delivered such a vaccine *via* the oral route of delivery (20).

MATERIALS

4T07 murine breast cancer cell line was a generous gift from Dr. Fred Miller, Barbara Ann Karmanos Cancer Institute, Detroit, MI. For *in vitro* cell culture, Dulbecco's modified Eagle medium (DMEM), Roswell Park Memorial Institute (RPMI) 1640 medium, Hanks balanced salt solution (HBSS), and Dulbecco's phosphate-buffered saline (DPBS, pH 7.2 ± 0.2, composed of potassium chloride, monobasic potassium phosphate, sodium chloride, and dibasic sodium phosphate) were purchased from Atlanta Biologicals, GA. Beta-cyclodextrin (Cavamax W7) was obtained as a sample from International Specialty Products Inc. (now Ashland Inc., NJ). Trehalose was obtained from Sigma-Aldrich, MO. Hydroxyl propyl methylcellulose acetate succinate (HPMCAS, AQOAT) and ethyl cellulose 30% *w/v* aqueous dispersion (Aquacoat®) were purchased from FMC Biopolymers, PA. AdminPatch® 1200 microneedle array with 1100-μm microneedle length was purchased from NanoBiosciences LLC. Calcein/Fluoresoft-0.35%® was obtained from Holles Laboratories, Inc., MA. Methylene blue dye was obtained from Eastman Kodak Company, NY. The Bio-Rad DC (detergent compatible) protein assay kit and trypan blue dye were obtained from Bio-Rad, CA. The IgG ELISA kit was purchased from Bethyl Laboratories, TX. IgG isotypes (IgG1 and IgG2a) and goat anti-mouse horseradish peroxidase (HRP)-linked secondary antibody were obtained from Sigma-Aldrich, MO, and Bethyl Laboratories, TX, respectively. TMB (tetramethylbenzidine) substrate was from BD Pharmingen, CA. Recombinant murine interleukins, IL-2 (5×10^6 units/mg), was purchased from Peprotech Inc., NJ.

Flow cytometry cell markers were purchased from eBioscience, CA. All other ingredients were of analytical grade.

METHODS

Whole Cell Lysate Preparation and Quantification

The whole cell lysate of the murine breast cancer cell line 4T07 was prepared using a hypotonic lysis buffer (10 mM Tris and 10 mM NaCl) and a series of freeze-thaw cycles as described in our previous studies (20,26,27). The whole cell lysate (WCL) thus obtained was stored at − 80°C for further use. The total protein concentration of the WCL was quantified using the Bio-Rad DC™ total protein assay. *Vaccine Microparticle Preparation and Characterization.* Vaccine particles were formulated using the WCL, β-cyclodextrin, ethyl cellulose 30% *w*/*v* suspension (Aquacoat®), trehalose, and hydroxyl-propyl methylcellulose acetate succinate (HPMCAS) as described previously (20). All the ingredients used to formulate these particles have been used for drug delivery *via* skin previously by several others (28–31). Briefly, all ingredients were dissolved in deionized water for the formulation. The pH of the resulting solution was neutralized with 1 N HCl, and then, WCL of 4T07 cells was added. The aqueous formulation matrix was maintained on ice and spray dried by one-step process using the Buchi B-191 mini spray dryer (Buchi Corporation, New Castle, DE) at inlet temperature 125°C, outlet temperature 80°C, 500 NL/h, and 2% spray flow feed rate (20 mL/h) of peristaltic pump, and nozzle diameter 0.7 mm. The formulated microparticles were stored at − 20°C in a desiccant chamber for further use. The spray-dried microparticles were analyzed for their particle size using Spectrex laser particle counter (Spectrex Corp., CA) and surface charge (zeta potential) using Malvern Zetasizer Nano ZS (Malvern Instruments, Worcs, UK). Loading efficiency was determined by Bio-Rad DC™ total protein assay by extracting the lysate in phosphate-buffered saline.

Visualization of Microchannels. To visualize the microchannels, they were stained with either methylene blue or with calcein dye (Fluoresoft-0.35%®) and observed by light and confocal microscope, respectively. For methylene blue staining, full-thickness murine skin was freshly excised from the animal and treated with AdminPatch® 1200 microneedle array. The microchannels were stained with 1% *w*/*v* methylene blue solution for a minute. Excess stain was wiped with a Kimwipe™ followed by an alcohol wipe. Stained microchannels were imaged with Canon PowerShot ELPH 180 digital camera. The treated skin samples were embedded in OCT medium in tissue embedding molds and frozen at − 80°C. The frozen skin sections were cryomicrotomed transversally using Microm HM505E cryostat (Thermo Scientific) with a thickness of 50 μm. These sections were obtained on glass slides and viewed under Leica DM750 light microscope using a Leica ICC50HD camera at ×10 and ×40 magnification. For confocal microscopy, full-thickness skin was freshly excised and treated with microneedles as described previously. The channels were then stained with Fluoresoft-0.35%®, for 2 min. Excess of dye was wiped similarly as described earlier (32). Full-thickness skin sections were obtained on a microscope slide and viewed under a Zeiss LSM510 confocal microscope with ×10 air objective. An argon laser of 488-nm wavelength was used to excite the fluorophore, and a band pass filter of 500–550 nm was used. The Z-stack image was obtained at a 10-μm step size, and an YZ section image was obtained to visualize the microchannels transversally. ImageJ software from the National Institute of Health, USA, was used to analyze the confocal images.

Immunization. The animal studies were conducted according to a protocol approved by Mercer University's Institutional Animal Care and Use Committee (IACUC). For the *in vivo* studies, 4 to 6-week-old Balb/c female mice, weighing approximately 22–24 g, were obtained from Charles River Laboratories (Wilmington, MA). Animals were divided into two groups: (a) vaccinated animals administered with 4T07 vaccine microparticles *via* microneedles and (b) control animals receiving no treatment ($n = 6$ for each group). All animals were pre-bled *via* tail vein to obtain basal antibody levels. For the vaccine delivery *via* skin, animal's back was shaved 24 h before the immunization. On the day of dosing, the immunization site was cleaned with an alcohol wipe and the AdminPatch® 1200 microneedle array was applied by placing the microneedle patch towards the skin, and applying a steady pressure using the thumb for 10 s. The patch was then removed, and 5 mg of vaccine particles suspended in 200 μL of citrate buffer (10 mM, pH 4.0) containing 200 mg/mL PEG 8000 (to enhance viscosity) was applied on the porated skin (33). The group (b) control animals remained untreated. One week after the prime dose, blood samples were collected from all the animals to analyze WCL-specific serum IgG antibody titers using ELISA. Five booster doses of the vaccine at the same strength were given at an interval of 2 weeks from the prior dose, and blood samples were collected a week after each dose to detect serum IgG levels. The booster doses were intended to potentiate the immune response by repeated exposure of the WCL every alternate week.

In Vivo Evaluation—Humoral Response. To perform antigen-specific ELISA, 4T07 whole cell lysate was used as the capture antigen coated on a 96-well plate at a concentration of 50 μg/mL/well. For detection of IgG, serum samples from the study were used to detect the IgG levels at a given time point. HRP-labeled secondary anti-mouse antibodies were used along with TMB substrate. The reaction was stopped by adding 4 N sulfuric acid, and the colored product was measured at 450 nm using a UV plate reader (BioTek Instruments Inc., VT). While for the detection of IgG1 and IgG2a, serum samples after the last boosters were used to determine IgG subtype titers (IgG1 and IgG2a). Rabbit anti-mouse isotype-specific antibodies were added to detect IgG1 and IgG2a, respectively. Further, a goat anti-rabbit secondary antibody labeled with HRP was used along with TMB substrate. The reaction was stopped with 4 N sulfuric acid, and the colored product was measured at 450 nm using a UV plate reader.

In Vivo Evaluation—Cellular Response. After the final booster, a subgroup of animals was euthanized as per Mercer

University IACUC protocol. Animals' abdominal cavities were excised open, and spleens of these animals were isolated aseptically. Spleen samples from animals in the same group were pooled and processed as described previously (20,27). Briefly, the spleens were gently reduced to a single cell suspension in RPMI-1640 media. Erythrocytes in this cell suspension were lysed and removed from the splenocytes. The splenocytes were suspended in complete RPMI-1640 media and stored at − 80°C till further use.

To identify the role of immune cells, splenocytes were cultured in complete RPMI-1640 media containing IL-2 (10 U/mL) for a day. 4T07 murine breast cancer cells were cultured in complete DMEM media separately and treated with mitomycin C (25 μg/mL for 10^7 cancer cells) for 30 min and then washed thrice. Both the cell populations were then co-cultured in the presence of IL-2 (10 U/mL)-enriched RPMI-1640 and DMEM media in 1:1 ratio. The co-culture was incubated for 3 days, and then, the stimulated splenocytes (non-adherent) were removed and quantified by trypan blue dye exclusion method using a Bio-Rad TC2 cell counter. This cell suspension was divided in the following equal parts based on the total viable cell count: (a) no markers were added to the first part; this served as the control for various cell populations to be analyzed; (b) anti-CD4+ PE (for T-helper cell) and anti-CD8+ FITC (for T-cytotoxic cell) markers; (c) anti-CD45R (B220) marker (for B cells); and (d) anti-CD161 marker (for NK cells). All the markers were added as per manufacturer's protocol. All the samples were incubated on ice for 30 min and subjected to analysis using BD Accuri® C6 flow cytometer (BD Accuri® Cytometers, MI) to analyze various cell populations in vaccinated and control groups.

Tumor Challenge. One week after the final booster, a subgroup of animals was challenged with 1×10^6 live 4T07 cells subcutaneously to determine the efficacy of 4T07 microparticulate vaccine given *via* the microneedles. Briefly, 4T07 cells were suspended in 100 μL of serum-free DMEM media and injected subcutaneously using a 25.5 gauge needle at the back and between the ears of each animal. Each animal was monitored for tumor growth weekly. Tumor growth was measured using Vernier calipers, and tumor volume was calculated according to the equation given below.

$$TumorVolume = \frac{1}{2}\left\{Length \times (Width)^2\right\}$$

Animals were observed for any signs of discomfort, and tumor burden was limited to a volume of 500–600 mm^3 or if the tumors became necrotic. Animals were sacrificed according to a protocol approved by Mercer University IACUC.

STATISTICAL ANALYSIS

All statistical analyses were performed using GraphPad Prism 7 (GraphPad Software, Inc., La Jolla, CA). Serum IgG and subtype titers, immune cell populations, and tumor volume measurements were analyzed using unpaired two-tailed Student's *t* test. For each test, the *p* value of less than 0.05 was considered significant. Data are expressed as a mean ± standard deviation.

RESULTS

Whole Cell Lysate Preparation and Quantification of Lysate. The whole cell lysate of 4T07 cells obtained by using hypotonic lysis buffer was a turbid mixture of TAAs. Since there is no known cell line–specific antigen identified at present to the best of our knowledge, the total protein concentration was analyzed to determine the antigen loading. The total protein concentration of WCL as obtained from 7 to 10×10^6 4T07 cells using a Bio-Rad DC total protein assay was 2.66 ± 0.5 mg/mL. This concentration was further utilized to quantify the volume of the lysate required for 5% *w*/*w* antigen loading in microparticle matrix and 50 μg/mL/well for ELISA studies as no specific antigens for the murine cell line were available.

Vaccine Microparticle Preparation and In Vitro Characterization of Microparticles. The yield of the microparticles obtained by the spray drying process was 77.21 ± 3.63% *w*/*w*. Particle size analysis indicated an average particle size of 1.54 ± 0.72 μm. Additionally as observed previously, the vaccine particles had an irregular donut surface morphology (20). Further, the zeta potential was neutral, ranging from 5.54 ± 1.62 mV. No significant change was found in size and charge upon loading these particles with the lysate. The loading efficiency of these particles was 90.18 ± 2.89% *w*/*w*. Thus, these particles were within the size range to mimic pathogenic species, thereby enhancing the potential of naturally being phagocytosed by the Langerhans cells (34,35). Thus, the uptake would allow processing of antigen-loaded microparticles leading to MHC presentations to the immune cells (36). These vaccine particles have also been successfully evaluated for their cell cytotoxicity in our previous studies (20). Briefly, the particles were non-cytotoxic for the tested concentration (0.0625–2 mg/mL) when evaluated in the presence of live RAW 264.7 macrophage cell line [studies evaluating beta-cyclodextrin particles report similar results elsewhere (30,37)].

Visualization of Microchannels. The efficacy of AdminPatch® 1200 microneedle array to breach skin was evaluated by staining the microchannels formed by the patch. The microchannels were formed by applying the patch on a freshly excised full-thickness murine skin. Further, the channels were stained using methylene blue and calcein dye and were observed under light and confocal microscope, respectively. The images from methylene blue and calcein staining are shown in Figs. 1 and 2, respectively. These images confirm the formation of microchannels and their specific dimensions. As shown in Fig. 1a, the microneedle array was successful in creating microchannels. Further, a transverse section of methylene blue–stained microchannels, as observed under Leica DM750 light microscope, shows the formation and morphology of the channel in Fig. 1b, c. Figure 1b provides a ×10 magnification view of the microchannel along with the remaining skin section, while Fig. 1c is a ×40 magnified view of one of the microchannels confirming that

these channels are approximately 50 μm deep. These images further potentiate the claim that the microchannels breach the skin barrier effectively but do not penetrate deep in the dermis where the blood vessels or nerve endings reside. The confocal microscopy images further supported the findings of methylene blue staining images. Figure 2a shows a Z-stack of calcein-stained microchannels on full-thickness murine skin as seen under a confocal microscope. In Fig. 2a, slice A (bottom right) of the stack represents the uppermost skin layer, and each consecutive slice (B through G) is 10 μm deeper from the previous one. The pores of stained microchannels are apparently visible in slices A through F, providing an estimated depth of 50–60-μm-deep channels, as imaged *via* a Z-stack. These results were also confirmed by a YZ/transverse sectional confocal image of calcein-stained microchannels. Figure 2b shows a YZ/transverse sectional image where the observed microchannel has a depth of 50 ± 10 μm confirming the prior results.

The murine skin has a 10-μm-thick epidermal layer, and the dermis can range between 200 and 400 μm depending upon species, strain, and gender (38). Thus, the 50 ± 10-μm microchannels created by the metal microneedles were deep enough to deliver approximately 1.5-μm vaccine particles in the vicinity of Langerhans cells within the skin layers. The Langerhans cells are responsible for activation of adaptive immune responses and can potentially generate memory response for the cancer antigens for future encounters, avoiding a chance of relapse.

In Vivo Evaluation—Humoral Response. Antibody/B cell response was evaluated by performing WCL-specific ELISA using the serum samples collected in between the vaccine booster doses. ELISA results confirm that the serum IgG levels were significantly higher in vaccinated animals when compared to the controls at the end of the fifth booster dose ($p < 0.001$) (Fig. 3). The elevated serum IgG concentrations against the 4T07 antigens confirm the activation of B cells and hence humoral response in the form of IgG titers triggered by the vaccine microparticles. Further, IgG subtypes, IgG1 and IgG2a, were analyzed to evaluate the possibility of Th2 response and/or Th1 response pathways, respectively, at the end of the dosing regimen. As shown in Fig. 4, serum IgG1 levels were the same for both the groups, but serum IgG2a titers were elevated in vaccinated mice when compared to the control ($p < 0.0001$). These titers indicate that vaccine particles resulted in an elevated Th1 response. The Th1 response is responsible for CD4+ T cell activation which in turn leads to activation of antigen-presenting cells and CD8+ T cells. Thus, the Th1 response is indicative of stimulation of cellular immune response generated by the particulate vaccine administered *via* the skin.

In Vivo Evaluation—Cellular Response. To evaluate cellular response generated by the vaccine microparticles, splenocytes were analyzed for the presence of T cells (CD8+ and CD4+), B cells, and NK cell populations *via* flow cytometry. As shown in Fig. 5a, b, CD8+ T cell populations were found to be elevated in the vaccinated mice when compared to the control group. In the case of CD4+ T cell titers, the vaccinated groups showed a significant rise in the levels of these cells as shown in Fig. 5c, d. Further, flow cytometry experiments confirmed that there are a significantly higher number of B cells in vaccinated animals compared to control animals as shown in Fig. 6a, b ($p < 0.0001$ in each case). However, the NK cell expression was the same for both the vaccinated and the control groups (Fig. 6c, d).

The *in vivo* cellular response as observed by the elevated expression of CD4+ and CD8+ T cells is in correlation with the humoral responses seen before. As shown earlier, when the serum samples were analyzed for IgG subtypes, IgG2a titers were found to be elevated in the case of vaccinated mice compared to the control group. This IgG2a titer increase in vaccinated animals was indicative of Th1 pathway activation which is, in turn, supported by the elevated levels of CD4+ and CD8+ T cells. Thus, the results obtained for CD4+ and CD8+ T cells by flow cytometric analysis of splenocytes potentiate the cellular activation *via* the IgG2a-mediated immune pathway, as observed in the humoral responses. Similarly, higher B cell counts for vaccinated animals compared to the control animals support the elevated IgG titers observed for this group. Overall, the results from the flow cytometric study substantiate the humoral as well as cellular immune response activation upon vaccination using the microparticles delivered *via* the skin.

Tumor Challenge. At the end of vaccination, both vaccinated and control group mice were challenged with a subcutaneous injection of 1×10^6 live 4T07 tumor cells to evaluate and compare the immune response activation by the microparticulate vaccine. The tumor volumes were measured every week using digital Vernier calipers. As shown in Fig. 7, the tumor developed rapidly in the control group, and by the end of the third week, the tumor volumes of the two groups were significantly different ($p < 0.001$). Vaccinated animals had approximately five times smaller tumors than the control animals. Vaccinated animals remained protected from the rapid tumor growth for longer intervals than the controls indicating that the vaccine efficiently generated a protective immune response against the murine breast cancer model.

The above tumor suppression response correlated well with the activation of humoral and cellular immune responses as confirmed by ELISA and flow cytometry analyses shown earlier. Activation of both arms of adaptive immunity supports the mechanism of action behind the anti-tumor activity of this microparticulate vaccine.

DISCUSSIONS

Several researchers have utilized whole cell lysates to formulate particulate vaccines and evaluate their immune response *in vivo* (39–43). Gross *et al*. successfully formulated and evaluated a microparticulate vaccine using 4T1 murine breast cancer cell lysate using poly(lactic-co-glycolic acid) (PLGA) dissolved in an organic solvent phase. This study utilized the double emulsion solvent evaporation technique to prepare the vaccine microparticles (39). On the contrast, our study provides an alternate technique to utilize polymers such as beta cyclodextrin, ethyl cellulose, and hydroxyl-propyl methylcellulose acetate succinate (HPMCAS) that can be

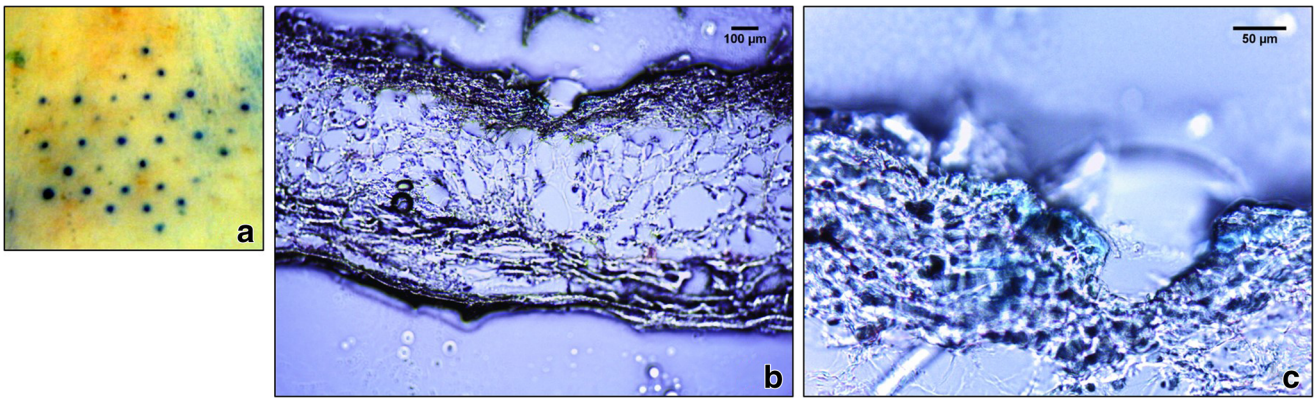

Fig. 1. Images of methylene blue–stained microchannels created using AdminPatch® 1200 metal microneedles. **a** Photograph representing porated murine skin stained with methylene blue as observed using Cannon digital camera. **b** Light microscopy images for a transverse histology section of microneedle-treated skin as seen under ×10 magnification with a Leica DM750 light microscope using Leica ICC50HD camera. **c** A ×40 magnification of the same section, observed with the same equipment

solubilized in an aqueous environment. Additionally, we demonstrate the application of the spray drying technique to prepare particulate vaccines. Spray drying technique is an established technique for commercial applications and can be conveniently scaled up. Lastly, this study also proposes an alternate route of administration for cancer vaccinations, thus collectively supporting the research in this direction along with other researchers in the field.

Overall, the current study successfully evaluated a particulate breast cancer vaccine delivered using microneedles. The breast cancer vaccine utilized a whole cell lysate of 4T07 murine cells as the source of TAAs. The whole

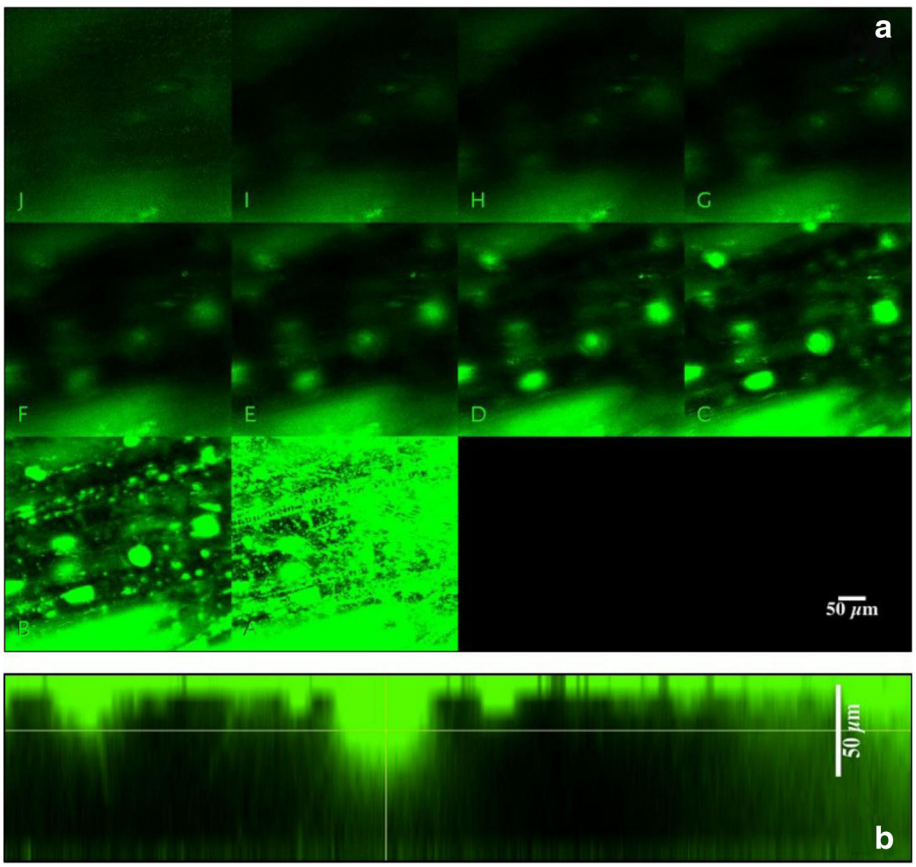

Fig. 2. Confocal images of calcein-stained microchannels created using AdminPatch® 1200 metal microneedles. **a** A Z-stack of calcein-stained microchannels. Calcein was observed in microchannels to up to 50 ± 10-μm depth. **b** An YZ section of a microchannel showing the depth of calcein permeation through the microchannel

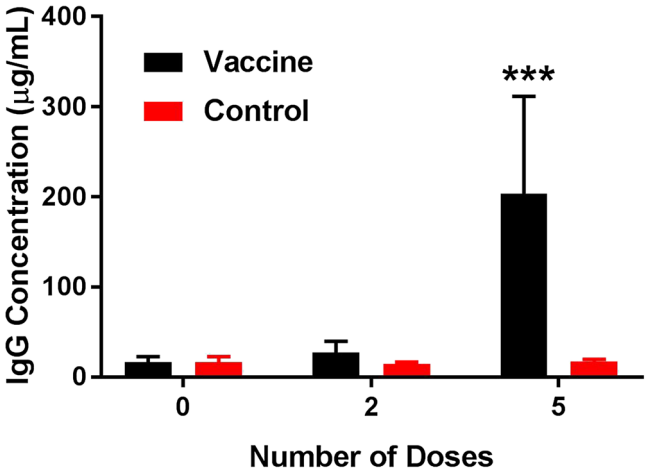

Fig. 3. *In vivo* humoral response: serum IgG titers of vaccinated and control animals after a series of booster vaccine doses. Vaccinated animals had significantly higher serum IgG titers after fifth booster dose compared to the control animals (***$p < 0.001$)

cell lysate was successfully entrapped in a microparticulate delivery system using the spray drying technology. The resulting particulate breast cancer vaccine had an average particle size of 1.5 μm, which mimics pathogenic species, thereby enhancing the potential of being recognized by the antigen-presenting cells. Such recognition leads to phagocytosis and antigen presentation *via* MHC pathways to activate the immune cells (3).

The antigen presentation further depends on the route of administration. Antigens have been delivered *via* the skin to elicit an immune response for several years now. Microneedles deliver these antigens in skin layers, allowing their uptake by the phagocytic cells (Langerhans cells) and further induction of immune response. Various proteins, genetic material (oligonucleotides, plasmid DNA), and live-attenuated viruses (influenza, Japanese encephalitis)

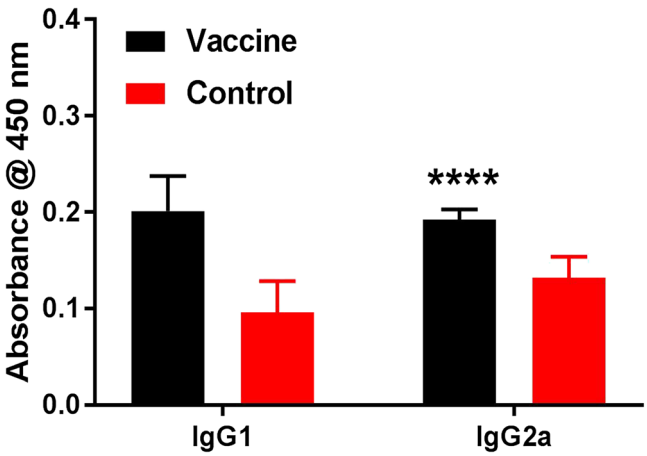

Fig. 4. *In vivo* humoral response: serum IgG1 and IgG2a titers of vaccinated and control animals post-immunizations. No statistical difference was observed in serum IgG1 titers between the two study groups. However, vaccinated animals had significantly higher serum IgG2a titers compared to the control animals (****$p < 0.0001$)

have been delivered *via* microneedles to evaluate their efficacy both *in vitro* and *in vivo* (44–47). Along with being efficacious, microneedle-based vaccination is associated with minimal pain and has proven to be safe both in human and animal studies (48–50). Therefore, this study was conducted to explore vaccine administration *via* skin using microneedles to create microchannels and deliver antigen load to activate the immune system. Characterization of microchannels was imperative here to understand the site of vaccine delivery and its impact on activation of the immune response. To visualize the microchannels created by AdminPatch® 1200 metal microneedle array, both methylene blue and calcein staining were performed. Methylene blue staining showed that the microneedle array was capable of piercing the murine skin and lead to the formation of aqueous channels which can be used for vaccine delivery. It showed that the stratum corneum of the skin was successfully breached and led to formation of an approximately 50-μm-deep channel. Confocal images of the channels further confirmed the depth of the microchannels *via* the Z-stack and YZ/transverse section images. The 50 ± 10-μm microchannels created by the metal microneedles were deep enough to deliver vaccine particles in the vicinity of Langerhans cells in the skin layers.

Further *in vivo* studies were conducted to evaluate the efficacy of microneedles to activate the immune response to the microparticulate vaccine. As evaluated *via* the *in vivo* studies, the 4T07 microparticulate vaccine was capable of eliciting serum IgG and IgG2a response, hence activating the Th1 pathway in vaccinated animals. Additionally, the vaccine activated both T-helper (CD4+) and T-cytotoxic (CD8+) along with B cell populations in comparison to controls. The cellular immunity responses are vital for an efficacious cancer vaccine as they lead to the antigen-specific immune responses thus limiting the potential of adverse effects (51). The resulting T-helper cells are responsible for activating naïve B cells and thereby lead to antibody production against the antigen-bearing cells. This was confirmed both by significant higher B cell populations and humoral response of higher serum IgG. Similar activation of Th1 pathway towards a murine breast cancer vaccine has been reported by Rainone *et al.* (42). Their study utilized dendritic cells pulsed with whole tumor lysate as a source of known and unknown antigens, in a murine breast cancer model (MMTV-Ras), and observed activation of immunocompetent cells and the release of Th1 cytokines as an anti-tumor response.

Overall, the vaccine exhibited both humoral and cellular responses against the cancer antigens. Upon completion of the vaccination, animals were challenged with 4T07 live murine breast cancer cells to determine the efficacy of the particulate vaccine delivered *via* the skin. Tumor volumes measured at the third week showed that the vaccinated animals had significantly smaller tumors when compared to the controls ($p < 0.001$). Tumor volume was retarded by five times in the case of vaccinated mice. This study indicated that the microparticulate vaccine administered *via* skin could exhibit humoral as well as a cellular immune response along with a significant tumor suppression in the vaccinated group.

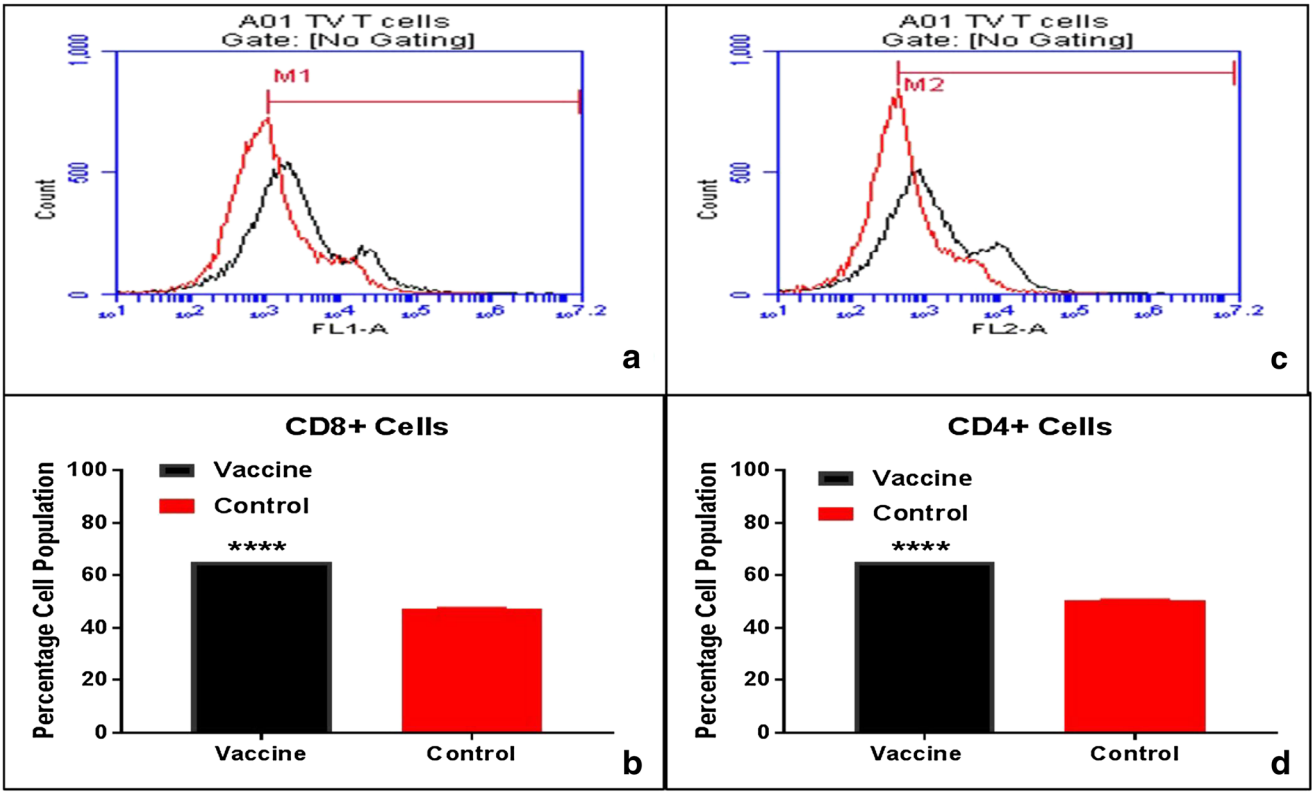

Fig. 5. *In vivo* cellular response: **a** CD8+ cell population of vaccinated animals (black) showing a shift towards the right compared to the controls (red). **b** The percentage cell population in the "M1" region denoted by the right side shift depicts significantly higher number of CD8+ T cells in vaccinated animals (****$p < 0.0001$). **c** CD4+ cell population in vaccinated animals (black) showing a shift towards the right compared to the controls (red). **d** The percentage cell population in the "M2" region denoted by the right side shift depicts significantly higher number of CD4+ T cells in vaccinated animals (****$p < 0.0001$)

This finding emphasizes the importance of humoral response in addition to a cellular response which is in alignment with the study reported by Mahmoud *et al.*, where it was found that the humoral immunity is important in addition to cell-mediated immunity in the prognosis of breast cancer (51). This overall stimulation of humoral and cellular response obtained upon vaccination reflects the overall immune response activation and hence the efficacy of vaccine particles. Additionally, the elevated immune response in vaccinated animals correlated well with the tumor suppression. Vaccination *via* skin was found to be protective as a route of administration for the particulate breast cancer vaccine. Microneedles can be effectively used to vaccinate *via* skin against breast cancer with the aid of particulate delivery systems as shown in this study using a murine model.

Further, here we also compare the immune activation as seen in our previously published study, where the 4T07 WCL vaccine microparticles were delivered orally (20). Both the studies utilize the same particulate vaccine at the same antigen dose for immune activation but use different routes of administrations (oral *vs*. *via* the skin). As described previously, orally delivered vaccine particles elicited humoral as well as cellular immune response and followed both Th1 and Th2 pathway. Tumor volume was suppressed 1.5 times when compared to controls upon oral vaccination. As shown in the study described above, the same vaccine particles rendered humoral as well as cellular immune response and exhibited Th1 pathway with tumor volume retardation by five times when compared to the control group. Moreover, tumor volumes observed post-vaccination and post-challenge with live cancer cells were significantly larger in orally vaccinated animals when compared to those observed in animals vaccinated *via* the skin at the end of 3 weeks ($p < 0.05$). These observations indicate the differences in vaccine delivery, challenges in immune activation, and immune pathways followed by the vaccine particles *via* the two different routes of administration. Vaccination *via* skin served to be a better route of immunization for the studied breast cancer model.

The study outcomes provide a novel research approach for individualized immunotherapy that may be utilized post-surgery. Breast cancer tumors isolated from such patients may provide a series of antigens to serve as TAAs to prepare an individualized cancer vaccine. Delivery of multiple boosters of such particulate cancer vaccines *via* skin will further support the application of this immunotherapy.

LIMITATIONS

Based on the scope of this study, the authors acknowledge three study limitations shared in this section. Firstly, the study utilizes one dose of the whole cell lysate vaccine to evaluate the immune response; future studies can be performed with varying antigen dose to quantify the dose delivered and its response thereof. Secondly, this study

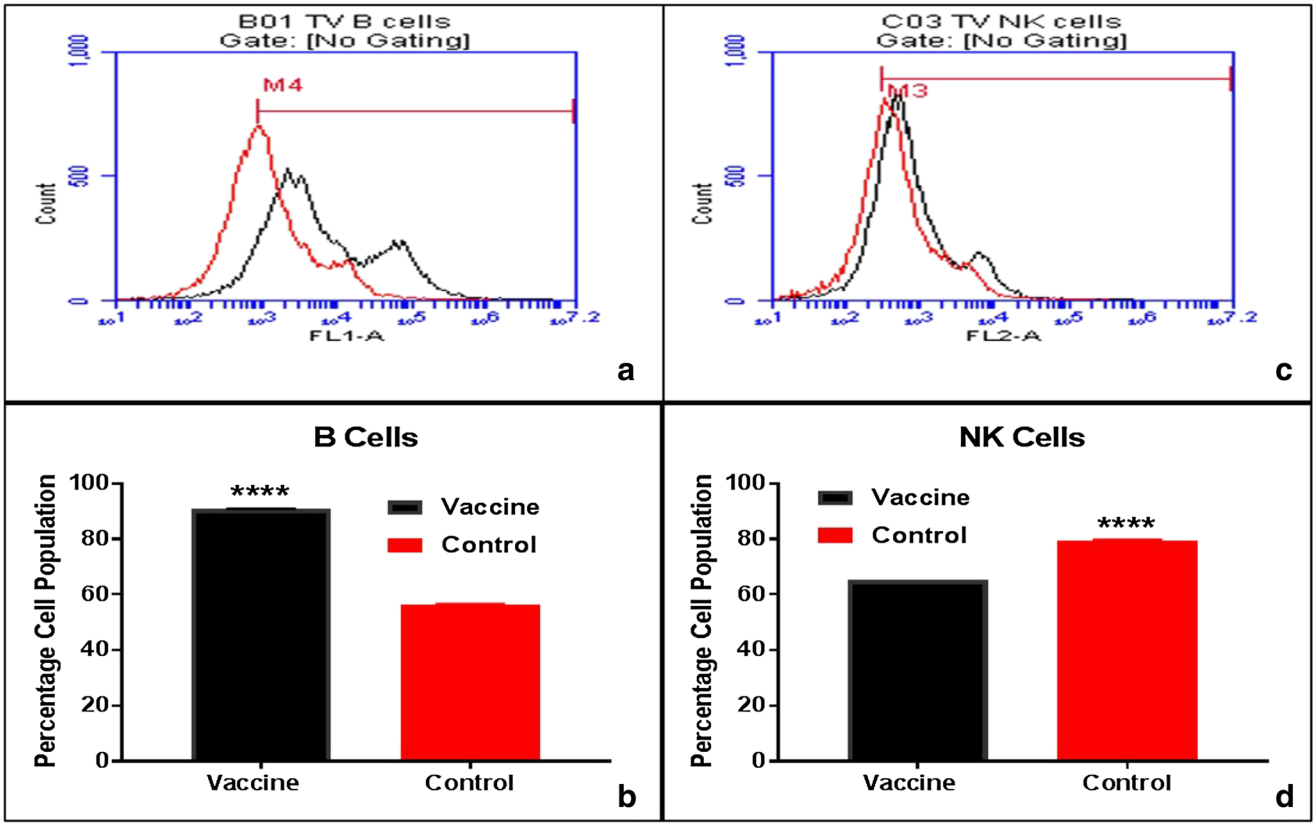

Fig. 6. *In vivo* cellular response: **a** B cell population in vaccinated animals (black) showing a shift towards the right compared to the controls (red). **b** The percentage cell population in the "M4" region denoted by the right side shift depicts significantly higher number of B cells in vaccinated animals (****$p < 0.0001$). **c** NK cell population in vaccinated animals (black) showing no shift compared to the controls (red). **d** The percentage cell population in the "M3" region denoted by the right side shift depicts significantly higher number of NK cells in control animals (****$p < 0.001$)

limits the *in vivo* evaluation of the immune response against the cancer antigens by quantifying the IgG, IgG1, IgG2a titers, T cell (CD4+ and CD8+), B cell, and NK cell populations. Further studies such as T cell/NK cell depletion studies were beyond the scope and can be performed in the future. Lastly, the antibody titers for IgG subtypes were evaluated at the end of the *in vivo* study at the given concentration only. This evaluation can benefit from a titration curve of further serial dilutions in the future.

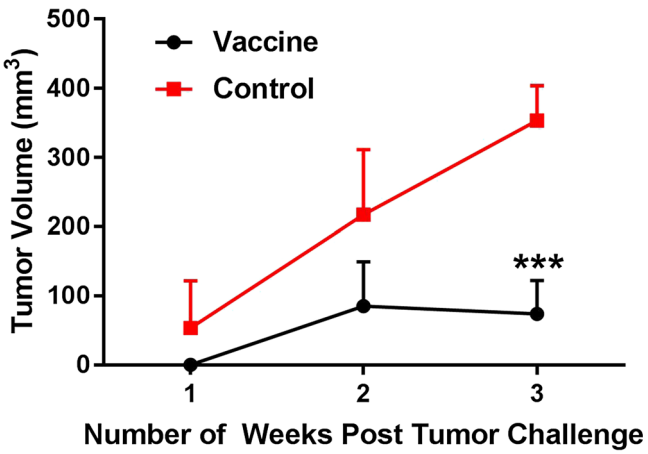

Fig. 7. Tumor challenge: tumor volumes for vaccinated and control animals weeks after challenge. Vaccinated animals had significantly smaller tumor volumes compared to the controls at the end of 3 weeks post-challenge with live 4T07 murine breast cancer cells (***$p < 0.001$)

CONCLUSIONS

The novel approach to formulating particulate breast cancer vaccines, which can be efficiently delivered *via* skin, proves to be a promising mode of immunization against breast cancer as shown by *in vivo* studies in this study. This mode of immunization can be used as an individualized therapy further as a therapeutic vaccine, where tumor cells can be isolated from the patient and cell homogenate can be formulated into a particulate vaccine to avoid relapse and enhance the immune response.

ACKNOWLEDGMENTS

This work was supported by Georgia Cancer Coalition grant. We would like to thank Dr. Fred Miller for providing the 4T07 murine breast cancer cell line.

COMPLIANCE WITH ETHICAL STANDARDS

Conflict of Interest The authors declare that they have no conflict of interest.

REFERENCES

1. Mittendorf EA, Alatrash G, Xiao H, Clifton GT, Murray JL, Peoples GE. Breast cancer vaccines: ongoing National Cancer Institute-registered clinical trials. Expert Rev Vaccines. 2011;10(6):755–74.
2. Mittendorf EA, Holmes JP, Ponniah S, Peoples GE. The E75 HER2/neu peptide vaccine. Cancer Immunol Immunother. 2008;57(10):1511–21.
3. Combadiere B, Mahe B. Particle-based vaccines for transcutaneous vaccination. Comp Immunol Microbiol Infect Dis. 2008;31(2–3):293–315.
4. Glenn GM, Taylor DN, Li X, Frankel S, Montemarano A, Alving CR. Transcutaneous immunization: a human vaccine delivery strategy using a patch. Nat Med. 2000;6(12):1403–6.
5. Mattheolabakis G, Lagoumintzis G, Panagi Z, Papadimitriou E, Partidos CD, Avgoustakis K. Transcutaneous delivery of a nanoencapsulated antigen: induction of immune responses. Int J Pharm. 2010;385(1–2):187–93.
6. Weldon WC, Martin MP, Zarnitsyn V, Wang B, Koutsonanos D, Skountzou I, et al. Microneedle vaccination with stabilized recombinant influenza virus hemagglutinin induces improved protective immunity. Clin Vaccine Immunol. 2011;18(4):647–54.
7. Yu RC, Abrams DC, Alaibac M, Chu AC. Morphological and quantitative analyses of normal epidermal Langerhans cells using confocal scanning laser microscopy. Br J Dermatol. 1994;131(6):843–8.
8. Al-Zahrani S, Zaric M, McCrudden C, Scott C, Kissenpfennig A, Donnelly RF. Microneedle-mediated vaccine delivery: harnessing cutaneous immunobiology to improve efficacy. Expert Opin Drug Deliv. 2012;9(5):541–50.
9. Hong X, Wei L, Wu F, Wu Z, Chen L, Liu Z, et al. Dissolving and biodegradable microneedle technologies for transdermal sustained delivery of drug and vaccine. Drug Des Devel Ther. 2013;7:945–52.
10. Naito S, Maeyama J, Mizukami T, Takahashi M, Hamaguchi I, Yamaguchi K. Transcutaneous immunization by merely prolonging the duration of antigen presence on the skin of mice induces a potent antigen-specific antibody response even in the absence of an adjuvant. Vaccine. 2007;25(52):8762–70.
11. Prausnitz MR, Mikszta JA, Cormier M, Andrianov AK. Microneedle-based vaccines. Curr Top Microbiol Immunol. 2009;333:369–93.
12. Sugita K, Kabashima K, Atarashi K, Shimauchi T, Kobayashi M, Tokura Y. Innate immunity mediated by epidermal keratinocytes promotes acquired immunity involving Langerhans cells and T cells in the skin. Clin Exp Immunol. 2007;147(1):176–83.
13. Gorse GJ, Falsey AR, Fling JA, Poling TL, Strout CB, Tsang PH. Intradermally-administered influenza virus vaccine is safe and immunogenic in healthy adults 18-64 years of age. Vaccine. 2013;31(19):2358–65.
14. Kim YC, Park JH, Prausnitz MR. Microneedles for drug and vaccine delivery. Adv Drug Deliv Rev. 2012;64(14):1547–68.
15. Atmar RL, Patel SM, Keitel WA. Intanza((R)): a new intradermal vaccine for seasonal influenza. Expert Rev Vaccines. 2010;9(12):1399–409.
16. Uppuluri C, Shaik AS, Han T, Nayak A, Nair KJ, Whiteside BR, et al. Effect of microneedle type on transdermal permeation of Rizatriptan. AAPS PharmSciTech. 2017;18(5):1495–506.
17. Nayak A, Das DB, Chao TC, Starov VM. Spreading of a lidocaine formulation on microneedle-treated skin. J Pharm Sci. 2015;104(12):4109–16.
18. Zhang D, Das DB, Rielly CD. Microneedle assisted microparticle delivery from gene guns: experiments using skin-mimicking agarose gel. J Pharm Sci. 2014;103(2):613–27.
19. Heppner GH, Miller FR, Shekhar PM. Nontransgenic models of breast cancer. Breast Cancer Res. 2000;2(5):331–4.
20. Chablani L, Tawde SA, Akalkotkar A, D'Souza C, Selvaraj P, D'Souza MJ. Formulation and evaluation of a particulate oral breast cancer vaccine. J Pharm Sci. 2012;101(10):3661–71.
21. Chiang CL, Benencia F, Coukos G. Whole tumor antigen vaccines. Semin Immunol. 2010;22(3):132–43.
22. Chiang CL, Kandalaft LE, Tanyi J, Hagemann AR, Motz GT, Svoronos N, et al. A dendritic cell vaccine pulsed with autologous hypochlorous acid-oxidized ovarian cancer lysate primes effective broad antitumor immunity: from bench to bedside. Clin Cancer Res. 2013;19(17):4801–15.
23. Cho DY, Yang WK, Lee HC, Hsu DM, Lin HL, Lin SZ, et al. Adjuvant immunotherapy with whole-cell lysate dendritic cells vaccine for glioblastoma multiforme: a phase II clinical trial. World Neurosurg. 2012;77(5–6):736–44.
24. Wolfraim LA, Takahara M, Viley AM, Shivakumar R, Nieda M, Maekawa R, et al. Clinical scale electroloading of mature dendritic cells with melanoma whole tumor cell lysate is superior to conventional lysate co-incubation in triggering robust in vitro expansion of functional antigen-specific CTL. Int Immunopharmacol. 2013;15(3):488–97.
25. Sosnik A, Seremeta KP. Advantages and challenges of the spray-drying technology for the production of pure drug particles and drug-loaded polymeric carriers. Adv Colloid Interf Sci. 2015;223:40–54.
26. Akalkotkar A, Tawde SA, Chablani L, D'Souza MJ. Oral delivery of particulate prostate cancer vaccine: in vitro and in vivo evaluation. J Drug Target. 2012;20(4):338–46.
27. Tawde SA, Chablani L, Akalkotkar A, D'Souza C, Chiriva-Internati M, Selvaraj P, et al. Formulation and evaluation of oral microparticulate ovarian cancer vaccines. Vaccine. 2012;30(38):5675–81.
28. Ammar HO, Salama HA, Ghorab M, El-Nahhas SA, Elmotasem H. A transdermal delivery system for glipizide. Curr Drug Deliv. 2006;3(3):333–41.
29. Idrees A, Rahman NU, Javaid Z, Kashif M, Aslam I, Abbas K, et al. In vitro evaluation of transdermal patches of flurbiprofen with ethyl cellulose. Acta Pol Pharm. 2014;71(2):287–95.
30. D'Souza B, Bhowmik T, Uddin MN, Oettinger C, D'Souza M. Development of beta-cyclodextrin-based sustained release microparticles for oral insulin delivery. Drug Dev Ind Pharm. 2015;41(8):1288–93.
31. Lee JW, Choi SO, Felner EI, Prausnitz MR. Dissolving microneedle patch for transdermal delivery of human growth hormone. Small. 2011;7(4):531–9.
32. Kalluri H, Kolli CS, Banga AK. Characterization of microchannels created by metal microneedles: formation and closure. AAPS J. 2011;13(3):473–81.
33. Bhowmik T, D'Souza B, Shashidharamurthy R, Oettinger C, Selvaraj P, D'Souza MJ. A novel microparticulate vaccine for melanoma cancer using transdermal delivery. J Microencapsul. 2011;28(4):294–300.
34. Reis e Sousa C, Stahl PD, Austyn JM. Phagocytosis of antigens by Langerhans cells in vitro. J Exp Med. 1993;178(2):509–19.
35. Morhenn VB, Lemperle G, Gallo RL. Phagocytosis of different particulate dermal filler substances by human macrophages and skin cells. Dermatol Surg. 2002;28(6):484–90.
36. Slutter B, Jiskoot W. Sizing the optimal dimensions of a vaccine delivery system: a particulate matter. Expert Opin Drug Deliv. 2016;13(2):167–70.
37. Dufour G, Bigazzi W, Wong N, Boschini F, de Tullio P, Piel G, et al. Interest of cyclodextrins in spray-dried microparticles formulation for sustained pulmonary delivery of budesonide. Int J Pharm. 2015;495(2):869–78.
38. Calabro K, Curtis A, Galarneau JR, Krucker T, Bigio IJ. Gender variations in the optical properties of skin in murine animal models. J Biomed Opt. 2011;16(1):011008.
39. Gross BP, Wongrakpanich A, Francis MB, Salem AK, Norian LA. A therapeutic microparticle-based tumor lysate vaccine reduces spontaneous metastases in murine breast cancer. AAPS J. 2014;16(6):1194–203.
40. Iranpour S, Nejati V, Delirezh N, Biparva P, Shirian S. Enhanced stimulation of anti-breast cancer T cells responses by dendritic cells loaded with poly lactic-co-glycolic acid

(PLGA) nanoparticle encapsulated tumor antigens. J Exp Clin Cancer Res. 2016;35(1):168.
41. Joshi VB, Geary SM, Gross BP, Wongrakpanich A, Norian LA, Salem AK. Tumor lysate-loaded biodegradable microparticles as cancer vaccines. Expert Rev Vaccines. 2014;13(1):9–15.
42. Rainone V, Martelli C, Ottobrini L, Biasin M, Texido G, Degrassi A, et al. Immunological characterization of whole tumour lysate-loaded dendritic cells for Cancer immunotherapy. PLoS One. 2016;11(1):e0146622.
43. Solbrig CM, Saucier-Sawyer JK, Cody V, Saltzman WM, Hanlon DJ. Polymer nanoparticles for immunotherapy from encapsulated tumor-associated antigens and whole tumor cells. Mol Pharm. 2007;4(1):47–57.
44. Birchall J, Coulman S, Pearton M, Allender C, Brain K, Anstey A, et al. Cutaneous DNA delivery and gene expression in ex vivo human skin explants via wet-etch micro-fabricated micro-needles. J Drug Target. 2005;13(7):415–21.
45. Chabri F, Bouris K, Jones T, Barrow D, Hann A, Allender C, et al. Microfabricated silicon microneedles for nonviral cutaneous gene delivery. Br J Dermatol. 2004;150(5):869–77.
46. Dean CH, Alarcon JB, Waterston AM, Draper K, Early R, Guirakhoo F, et al. Cutaneous delivery of a live, attenuated chimeric flavivirus vaccine against Japanese encephalitis (ChimeriVax)-JE) in non-human primates. Hum Vaccin. 2005;1(3):106–11.
47. Mikszta JA, Sullivan VJ, Dean C, Waterston AM, Alarcon JB, Dekker JP 3rd, et al. Protective immunization against inhalational anthrax: a comparison of minimally invasive delivery platforms. J Infect Dis. 2005;191(2):278–88.
48. Gill HS, Denson DD, Burris BA, Prausnitz MR. Effect of microneedle design on pain in human volunteers. Clin J Pain. 2008;24(7):585–94.
49. Kaushik S, Hord AH, Denson DD, McAllister DV, Smitra S, Allen MG, et al. Lack of pain associated with microfabricated microneedles. Anesth Analg. 2001;92(2):502–4.
50. Mikszta JA, Alarcon JB, Brittingham JM, Sutter DE, Pettis RJ, Harvey NG. Improved genetic immunization via micromechanical disruption of skin-barrier function and targeted epidermal delivery. Nat Med. 2002;8(4):415–9.
51. Mahmoud SM, Lee AH, Paish EC, Macmillan RD, Ellis IO, Green AR. The prognostic significance of B lymphocytes in invasive carcinoma of the breast. Breast Cancer Res Treat. 2012;132(2):545–53.